Sensors and Materials, Vol. 37, No. 8 (2025) 3697–3706
MYU Tokyo

S & M 4146

Multilayer Metamaterial-based Absorber with Ultra-wideband Performance from Visible to Mid-infrared Range

Lin Wang,[1] Chia-Min Ho,[2] Chin-Ta Chen,[1] Cheng-Fu Yang,[2,3*] and Kao-Wei Min[4**]

[1]School of Electronic and Electrical Engineering, Zhaoqing University, Zhaoqing 526061, China
[2]Department of Chemical and Materials Engineering, National University of Kaohsiung, Kaohsiung 811, Taiwan
[3]Department of Aeronautical Engineering, Chaoyang University of Technology, Taichung 413, Taiwan
[4]Department of Electrical Engineering, Cheng Shiu University, Kaohsiung 833, Taiwan

(Received June 22, 2025; accepted August 6, 2025)

Keywords: multilayer, metamaterial-based absorber, ultra-wideband, visible, mid-infrared

An absorber capable of operating across the visible to mid-infrared spectrum holds tremendous promise for a wide range of sensor applications, including thermal imaging, environmental monitoring, infrared stealth, and broadband photodetection. In this study, we present the design of a high-performance multilayer metamaterial-based absorber that achieves ultra-wideband absorption through a carefully optimized layered structure. The absorber comprises a vertically stacked configuration consisting of alternating metallic and dielectric layers. From bottom to top, the structure includes an iron (Fe) substrate, followed by an h1 Fe layer (substrate), h2 Cu_2O layer, h3 Fe layer, h4 Cu_2O layer, h5 Fe layer, and h6 Cu_2O layer, and a topmost h7 Ti cylindrical matrix array. This design combines lossy metal layers with dielectric spacers to generate strong plasmonic resonances and constructive interference across a broad spectrum. Fe provides high intrinsic loss and low-cost fabrication, while Cu_2O acts as the dielectric layer to enhance field confinement and improve impedance matching. A patterned Ti cylindrical array on the top surface creates localized surface plasmon resonances and scatters light into the structure, further increasing absorption. Simulations show that the absorber achieves high absorptivity over a wide wavelength range, from around 620 nm in the visible to 7200 nm in the mid-infrared. The results highlight the potential of this multilayer metamaterial design for integration into next-generation optoelectronic and sensing systems requiring compact, efficient, and broadband light absorption.

1. Introduction

Near-infrared (NIR, 0.75–1.4 μm) and mid-infrared (MIR, 1.4–8 μm) absorbers serve as critical components across diverse engineering applications. NIR absorbers demonstrate significant utility in biomedical imaging and diagnostic systems owing to their ability to facilitate tissue penetration while maintaining high imaging fidelity, enabling their integration into various medical diagnostic platforms.[(1)] MIR absorbers find extensive implementation in

*Corresponding author: e-mail: cfyang@nuk.edu.tw
**Corresponding author: e-mail: 8373@gcloud.csu.edu.tw
https://doi.org/10.18494/SAM5827

ISSN 0914-4935 © MYU K.K.
https://myukk.org/

Fourier transform infrared (FTIR) spectroscopy systems for molecular structure identification and chemical analysis applications.[2] These devices also play a key role in environmental monitoring by detecting and measuring atmospheric gases and pollutants such as methane and carbon monoxide. Their ability to detect and image short-wave infrared (SWIR) light is essential for important applications such as biological imaging, autonomous navigation, and surveillance.[3] In biological imaging applications, SWIR light demonstrates superior tissue penetration characteristics while maintaining high-resolution imaging capabilities, making it invaluable for medical diagnostic and research applications.[4] Within autonomous navigation systems, SWIR sensors provide enhanced visibility performance across various environmental conditions, thereby improving operational reliability and safety parameters for autonomous vehicle platforms.[5] Surveillance applications benefit from SWIR imaging technology through effective monitoring and detection capabilities under low-light or visually obscured conditions, significantly enhancing security systems and situational awareness capabilities.[6]

Consequently, the development of high-performance infrared (IR) absorbers enables their integration into a broad spectrum of sensor technologies with diverse functional requirements and application domains.[7,8] Using iron (Fe) as the metallic component in absorbers designed for the visible (VIS) to MIR spectrum offers several key advantages. Fe has high optical loss in this range, allowing it to efficiently convert light into heat and improve overall absorption. This makes it ideal for broadband absorber designs. Additionally, Fe has good electrical conductivity and strong electromagnetic loss in the IR region, which helps with impedance matching, reduces reflection, and enhances energy absorption. Fe is also thermally and structurally stable, making it suitable for high-temperature applications. This makes it a viable material for applications such as solar thermal devices, IR detectors, and high-temperature sensors. Moreover, Fe forms stable and compatible heterostructures with various oxides, including Cu_2O, SiO_2, and Al_2O_3, which is beneficial for constructing multilayer interference or surface plasmon polariton (SPP) structures. These features collectively contribute to enhanced light confinement and absorption, reinforcing Fe's suitability as a core material in broadband absorber design.

The use of Cu_2O as the dielectric material in the design of an absorber spanning the VIS–MIR spectrum offers several critical advantages that enhance broadband absorption performance. Cu_2O possesses a relatively high refractive index ($n \approx 2.5$–3 in the VIS to NIR range), which facilitates stronger light confinement, enhances interference effects, and improves impedance matching with adjacent metallic layers. These properties contribute to reduced reflection and significantly increased light absorption. In addition, Cu_2O exhibits excellent optical transparency across the VIS–MIR range, particularly demonstrating low extinction coefficients in the MIR region. This low optical loss makes it highly suitable for multilayer interference or resonant structures, enabling effective light manipulation without excessive absorption or scattering. As a p-type semiconductor with a moderate direct bandgap (~2.0–2.2 eV), Cu_2O can form stable metal–semiconductor interfaces when paired with metallic layers. In certain designs, this structure may also support hot carrier effects, further improving the conversion of light into energy. Cu_2O plays an active role in multiple absorption mechanisms, including interference-based absorption, surface plasmon polaritons (SPPs), and localized surface plasmon resonances. These effects work together to enable strong absorption over a wide wavelength range, making it well-suited for high-performance, ultra-wideband absorbers.

In this study, we designed and analyzed a multilayer metamaterial absorber capable of covering a broad spectral range from 640 to 7140 nm. The seven-layer structure presented in this paper was originally designed by our research team and has not been directly reported elsewhere to the best of our knowledge. While previous studies have explored the individual roles of materials such as Fe, Cu_2O, and Ti in enhancing absorption in the VIS to MIR regions, the specific combination and arrangement of these materials into a seven-layer configuration is our own novel approach, aiming to synergistically optimize light absorption. The proposed absorber achieves high performance through three key innovations. First, it uses low-cost, widely available materials, namely, Cu_2O and metals such as Fe and Ti, instead of expensive noble metals such as Ag and Au. Cu_2O is especially important for controlling light behavior within the structure. With its adjustable refractive index and favorable optical properties, Cu_2O helps guide electromagnetic waves by affecting reflection and refraction, leading to better light trapping and enhanced absorption across the spectrum. Furthermore, Cu_2O serves as a low-reflectance layer, reducing optical losses at the surface and facilitating greater light transmission into the structure. Fe is utilized for its excellent electrical conductivity and intrinsic light absorption capability. It efficiently converts incident light into thermal energy, particularly in the VIS and MIR ranges. Additionally, Fe can support surface plasmon resonance effects at specific wavelengths, further amplifying absorption in the MIR region. Ti, especially when used as a thin film, exhibits strong absorption in the VIS and UV spectra. When integrated with other materials such as Cu_2O, it can generate unique interfacial effects that enhance absorption at selected wavelengths. Taken together, the synergistic combination of Cu_2O, Fe, and Ti enables the design of a broadband, high-performance optical absorber using economical and accessible materials.

2. Methodology

The detailed geometric configuration of the unit cell with a periodicity of $w_1 = 300$ nm for the proposed multilayer metamaterial absorber is illustrated in Fig. 1, showcasing a precisely engineered seven-layer architecture. In this design, Fe, Cu_2O, and Ti were chosen on the basis of their optical and physical properties, which were taken from the built-in COMSOL material database to ensure accurate simulations. Structural asymmetry was introduced by varying the lateral dimensions, helping improve impedance matching and light confinement over a wide spectral range. All simulations and structural analyses were carried out using COMSOL Multiphysics® (version 6.0), a commercial finite element analysis tool. A systematic parametric sweep was used, where one geometric parameter was adjusted at a time while keeping the others fixed. This approach enabled a detailed evaluation of how specific geometric modifications affect the absorber's optical performance and electromagnetic response. The primary objective of this study was to determine the optimal configuration of structural parameters that would achieve maximum absorption efficiency across the targeted wavelength range, while ensuring practical manufacturability and design feasibility. The investigated absorber employed a mesh structure with 25225 grid nodes, featuring a minimum grid length of 0.85 nm and a maximum of 1.68 nm. The mesh comprised 118379 tetrahedral elements, 13280 triangular elements, 57 endpoint elements, and 1145 edge elements. Mesh quality was evaluated with an average element

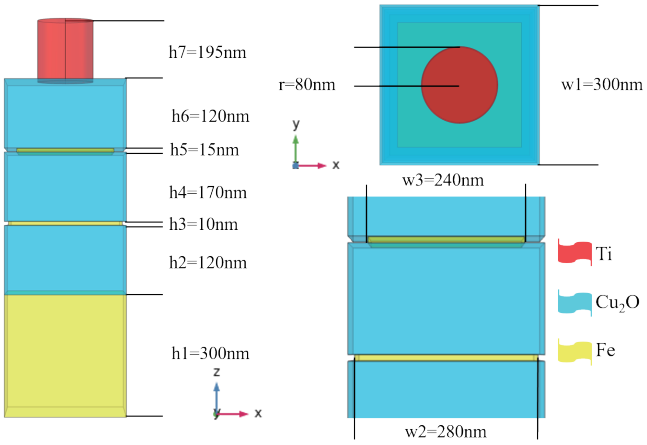

Fig. 1. (Color online) Side view and diameters of the unit cell of the investigated metamaterial-based absorber.

quality of 0.6478 and a minimum quality of 0.1625. The total grid volume was 2.05×10^8 nm^3, with an element volume ratio of 0.004687. This high-resolution mesh ensured both the reliability and accuracy of the simulation results.

3. Simulation Results and Discussion

We first analyzed the effect of the thickness of the h1 layer. The results showed that when the thickness of h1 increased from 260 to 340 nm, the absorption spectrum remained unchanged, with absorptivity exceeding 0.900 consistently within the wavelength range of 625–7100 nm (not shown here). This indicates that the thickness of the h1 layer has a minimal effect on the overall absorption performance. Therefore, the h1 layer thickness was fixed at 300 nm for subsequent design considerations. Figure 2(a) shows results of a detailed investigation into the impact of varying the thickness of the h2 Cu_2O layer on the absorptivity spectrum of the designed absorber. In this parametric study, the thickness of the h_2 layer was systematically adjusted while keeping all other geometric parameters constant, such as the thicknesses and widths of the remaining layers. The results demonstrate a strong dependence of absorptivity on the thickness of the Cu_2O layer. Two significant trends were observed as the h_2 thickness increased from 70 to 170 nm:

(1) Broadband Enhancement: The absorption bandwidth characterized by absorptivity values consistently exceeding 0.900 expanded significantly.
(2) Spectral shift: The high-absorptivity wavelength range shifted from approximately 650–6250 nm at h_2 = 80 nm to 650–7750 nm at h_2 = 160 nm.

These findings indicate that increasing the thickness of the h2 Cu_2O layer effectively extends the upper limit of the absorption spectrum while maintaining high absorptivity across a broader range. This behavior underscores the critical role of the Cu_2O layer in governing the optical response of the absorber, particularly in the mid- to long-wave IR regions. Overall, Fig. 2 highlights the importance of precise control over nanofilm thicknesses in optimizing the

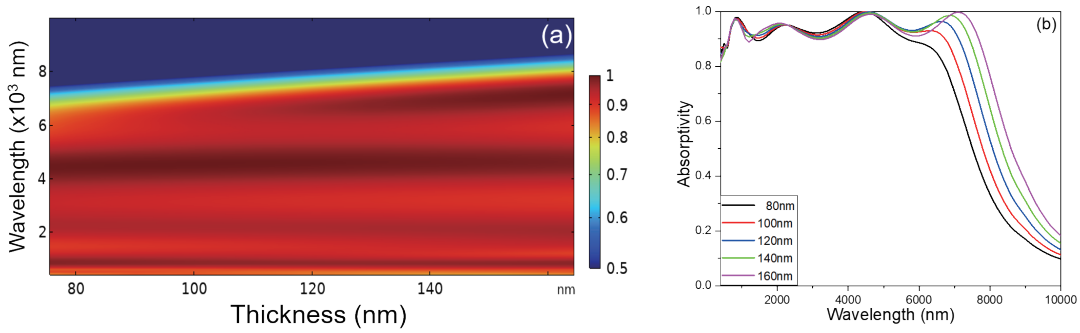

Fig. 2. (Color online) Effects of different wavelengths and different thicknesses of h2 Cu_2O layer on the (a) absorptivity distributions and (b) absorption spectra of the investigated absorbers.

performance of ultra-broadband optical absorbers. The ability to fine-tune the spectral range through structural adjustments provides valuable insight for the development of high-efficiency photonic and optoelectronic devices.

To gain a more comprehensive understanding of the effect of the h2 Cu_2O layer on the absorption characteristics, Fig. 2(b) illustrates the variation in the absorption spectrum as the thickness of the h2 layer is adjusted within the range of 80–160 nm. Increasing the thickness of the h_2 Cu_2O layer causes a redshift in the long-wavelength cutoff, extending absorption into the IR region. Closer analysis of the absorption dips around 1400 and 3200 nm shows that thinner h_2 layers fail to maintain high absorptivity, with values dropping below 0.900. Only when the thickness reaches 120 nm does the absorber achieve absorptivity above 0.900 in both regions. This indicates that 120 nm is an optimal thickness for strong and consistent absorption, especially in the NIR and MIR range. The observed redshift with increasing thickness can be attributed to the enhanced optical path length and interference effects within the Cu_2O layer. Thicker layers support more pronounced resonant modes, which shift the absorption peaks toward longer wavelengths. Additionally, Cu_2O's high refractive index and suitable bandgap make it particularly effective in tailoring the spectral response for broadband absorption when its thickness is properly optimized.

Figure 3(a) shows the significant impact of varying the thickness of the h3 Fe layer on the absorptivity spectrum across a wide range of wavelengths. The study systematically explores how changing the h3 Fe layer thickness within the 5–20 nm range affects absorption characteristics, while keeping all other layer thicknesses and widths constant. The simulation results reveal a strong correlation between the h3 Fe layer thickness and the absorber's spectral performance. As shown in Fig. 3(b), increasing the thickness of the h3 Fe layer produces two notable effects.

(1) When the thickness increases from 6 to 10 nm, the absorption bandwidth with absorptivity exceeding 0.900 expands significantly from approximately 5800 to 7250 nm.
(2) When the thickness exceeds 15 nm, the high-absorptivity bandwidth (above 0.900) suddenly contracts, dropping sharply from approximately 7250 to around 4800 nm.

These results suggest that the optimal thickness of the h3 Fe layer is 10 nm. This behavior suggests that while a moderate increase in Fe layer thickness enhances light absorption in the

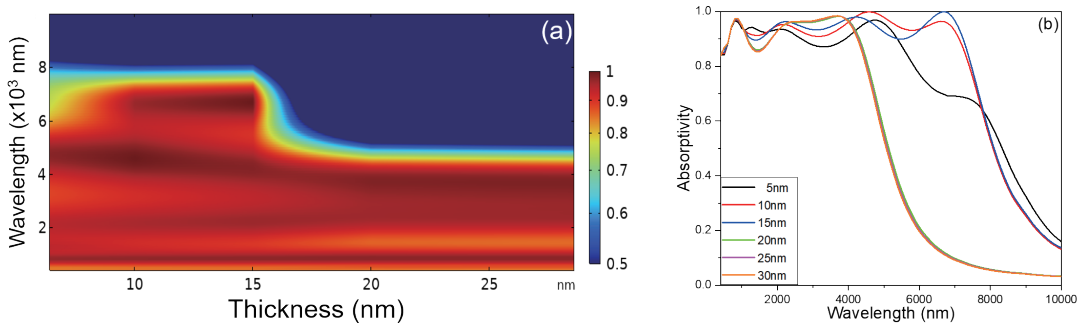

Fig. 3. (Color online) Effects of different wavelengths and different thicknesses of h3 Fe layer on the (a) absorptivity distributions and (b) absorption spectra of the investigated absorbers.

long-wavelength region, excessive thickness introduces adverse effects, possibly due to increased reflection losses or impedance mismatch. The optimal thickness range is therefore critical to maintaining strong coupling between the incident electromagnetic waves and the absorber structure. These findings underscore the essential role of the h3 Fe layer in tuning the absorption bandwidth and optimizing the device for ultra-broadband absorption, particularly in the MIR to long-IR region. They also highlight the necessity of finely tuning structural parameters to achieve maximal performance in multilayer optical absorber designs.

The designed absorber structure is composed of multiple stacked layers arranged from bottom to top as follows: an Fe substrate layer, h2 Cu_2O layer, h3 Fe layer, h4 Cu_2O layer, h5 Fe layer, and h6 Cu_2O layer, and a top layer consisting of a Ti cylindrical array. Figure 4 shows the effects of varying the thickness of the h4 Cu_2O layer on the absorptivity distribution across different wavelengths. As shown in the figure, changes in the h4 Cu_2O layer thickness result in a negligible variation in the spectral bandwidth exhibiting high absorptivity, indicating that this layer plays a relatively minor role in tuning the overall optical response. A similar trend is observed for the h6 Cu_2O layer, where thickness variations also have a limited impact on the absorptivity profile. Consequently, detailed results for the h6 layer are not shown here. In contrast, the h2 Cu_2O layer, positioned closer to the Fe substrate, has a more significant effect on the absorptivity distribution. Variations in its thickness strongly affect the spectral shape and the bandwidth of high absorptivity, likely due to its role in initial light–matter interaction and field enhancement effects near the substrate interface. Through simulation analysis, the optimal thicknesses of the h4 and h6 Cu_2O layers were determined to be 170 and 120 nm, respectively.

Furthermore, we conducted a comprehensive analysis of the effect of the h5 Fe layer thickness on optical absorption characteristics. As shown in Fig. 5(a), distinct spectral features emerge with changes in h5 thickness. When the h5 Fe layer was thinner than 12 nm, regions of low absorptivity (<0.900) appeared within the 800–1300 nm and beyond 3800 nm wavelength ranges, indicating that an ultrathin Fe layer significantly reduces absorption efficiency in these bands. As the h5 thickness increased, the high-absorptivity region expanded and reached saturation at 17 nm. However, when the thickness exceeded 17 nm, a new low-absorption region emerged near 3500 nm and progressively widened with further increases in thickness. To achieve a more detailed understanding of this behavior, we performed spectral scanning analysis

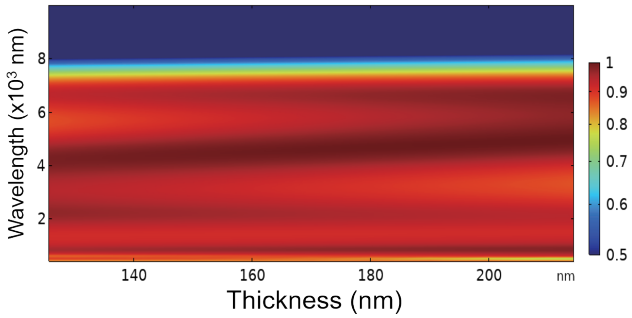

Fig. 4. (Color online) Effects of different wavelengths and different thicknesses of h4 Cu_2O layer on the absorptivity distributions of the investigated absorbers.

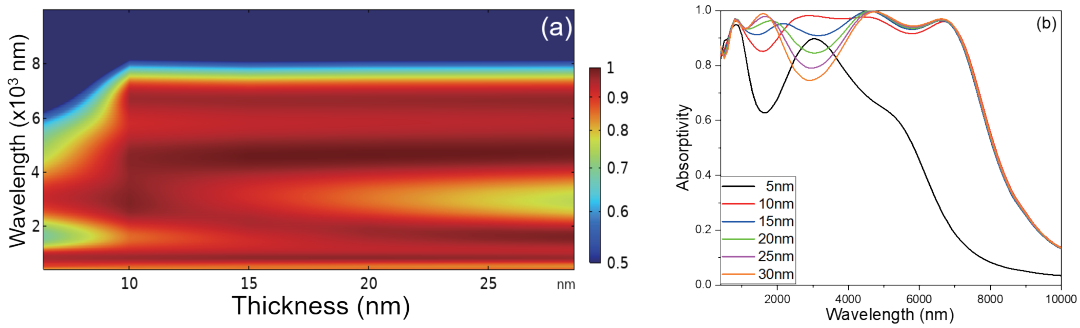

Fig. 5. (Color online) Effects of different wavelengths and different thicknesses of h5 Fe layer on the (a) absorptivity distributions and (b) absorption spectra of the investigated absorbers.

across the 200–10000 nm range, varying the h5 Fe layer thickness in 5 nm increments from 5 to 30 nm. The results are presented in Fig. 5(b). At 5 nm thickness, a pronounced low-absorption valley was observed around 1800 nm. As the thickness increased to 15 nm, this valley disappeared, and the absorptivity across the spectrum improved.

However, beyond 15 nm, the emergence and expansion of new low-absorption regions were observed, accompanied by a gradual decrease in overall absorptivity. On the basis of these findings, we conclude that a thickness of 15 nm offers the optimal balance for the h5 Fe layer, maximizing broadband absorption performance. These findings reveal a clear trade-off in the design of the h5 Fe layer: while increased thickness initially enhances broadband absorption due to improved light–matter interaction and potential resonance effects, excessive thickness introduces parasitic losses and unwanted reflective behavior in longer wavelengths. Therefore, a thickness of 15 nm is identified as the optimal value, offering a balanced performance by maximizing absorptivity across both VIS and IR regions without incurring additional spectral degradation. This demonstrates the critical role of precise nanometric tuning in multilayer absorber designs, where even small thickness variations can markedly affect the optical response due to interference, plasmonic, and field coupling effects.

These findings highlight the structure's promising potential for a variety of optical applications, such as photovoltaic devices and optical sensing systems. Compared with

previously reported designs, the proposed seven-layer structure demonstrates significantly enhanced absorption across the VIS to MIR spectrum, which is critical for broad-spectrum solar energy harvesting and photodetection. The integration of materials in a strategically multilayer configuration allows for efficient light trapping. These improvements suggest that the proposed design can lead to more sensitive photodetectors and more efficient photovoltaic devices in practical implementations. Notably, the presence of discontinuous cylindrical Ti elements appears to exert a substantial regulatory effect on the light absorption process. This may be attributed to multiple underlying physical mechanisms, including localized surface plasmon resonances, scattering-induced light trapping, and modulation of the local electromagnetic field distribution. Such interactions contribute to the dynamic and tunable optical behavior of the absorber, especially within the UV–VIS spectrum. Figures 6(a) and 6(b) illustrate the absorptivity distributions and corresponding absorption spectra, revealing that the incorporation of a discontinuous cylindrical Ti matrix results in significant optical responses across a broad wavelength range of 300 to 2200 nm. First, the diameter of cylindrical Ti was set at 160 nm. When the thickness of the h7 Ti layer is increased from 115 to 195 nm, a noticeable trade-off in absorption behavior is observed: the absorption peak in the 500–800 nm region decreases from near-perfect absorptivity (0.999) to 0.967, whereas the absorption valley in the 1000–1300 nm range improves markedly, with absorptivity increasing from 0.784 to 0.915. This trend indicates that tuning the thickness of the cylindrical Ti matrix provides an effective mechanism for modulating optical absorption, particularly enhancing light capture in the NIR and VIS regions.

The results suggest that the discontinuous cylindrical Ti matrix plays a critical role in tailoring the photonic response, offering a balance between high absorptivity at shorter wavelengths and enhanced performance in the NIR range. These findings highlight the structure's promising potential for a variety of optical applications, such as photovoltaic devices and optical sensing systems. Notably, the presence of the discontinuous cylindrical Ti elements appears to exert a substantial regulatory effect on the light absorption process. This may be attributed to multiple underlying physical mechanisms, including localized surface plasmon resonances, scattering-induced light trapping, and modulation of the local electromagnetic field distribution. Such interactions contribute to the dynamic and tunable optical behavior of the absorber, especially within the UV–VIS spectrum. The analysis results indicate that the optimal

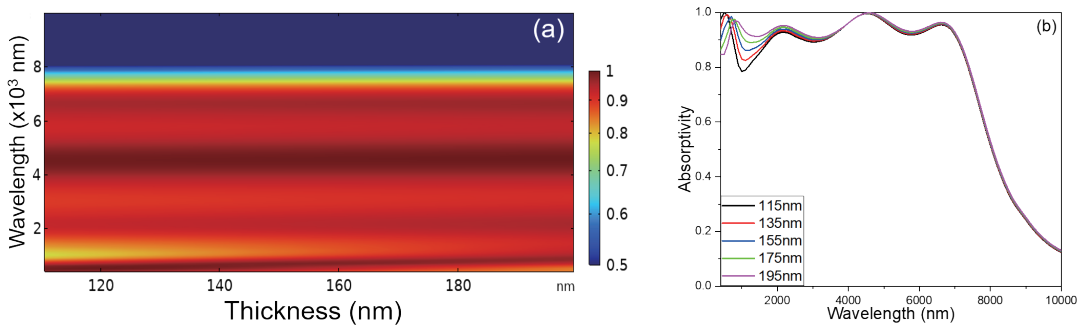

Fig. 6. (Color online) Effects of different wavelengths and different thicknesses of h7 Ti layer on the (a) absorptivity distributions and (b) absorption spectra of the investigated absorbers.

configuration of the proposed ultra-wideband absorber includes a 300-nm-thick h1 Fe layer at the base, functioning as a reflective substrate. Above this, alternating layers of Cu_2O and Fe are arranged to manipulate light propagation and enhance absorption. The h2, h4, and h6 Cu_2O layers have thicknesses of 120, 170, and 120 nm, respectively, each extending laterally to a width of 300 nm to match the unit cell periodicity. The intermediate h3 and h5 Fe layers are configured with thicknesses of 10 and 15 nm and lateral widths of 280 and 240 nm, respectively.

As shown in Fig. 6(b), the ultra-wideband optical absorber is specifically engineered to achieve high absorptivity across a broad spectral range, extending from the VIS region (600 nm) to the MIR region (7250 nm). The absorption spectrum presented in Fig. 6 exhibits four prominent absorption peaks located at 800, 2200, 4600, and 6600 nm. Accordingly, these wavelengths were selected for the simulation of the electric and magnetic field distributions, as depicted in Figs. 7(a) and 7(b), respectively. To compare the absorption characteristics, the primary focus is on observing the color variation at each position. Blue indicates a low-absorptivity area, whereas red represents a high-absorptivity area. Taking Fig. 7(b) as an example, at wavelengths of 800 and 2200 nm, the red region extends from the top layer down to the upper part of the bottom layer, indicating high absorption throughout this entire region. At wavelengths of 4600 and 6600 nm, a similar red distribution is observed; however, the Ti region appears green. This result confirms that Ti exhibits better absorption performance at shorter wavelengths. The results reveal strong absorption at 800 and 2200 nm, primarily due to the top Ti cylindrical layer, whereas reduced absorption is observed at 4600 and 6600 nm. These observations reinforce the earlier conclusion that the Ti cylindrical structure plays a critical role in enhancing absorption in the shorter wavelength range. As illustrated in Fig. 7(a), the strong localization of the electric field at shorter wavelengths correlates with higher absorption efficiency. Furthermore, as the wavelength increases, the regions of maximum electric field intensity gradually shift upward toward the top layers of the absorber. This spatial transition is consistent with the wavelength-dependent behavior of surface plasmon resonances, which exhibit stronger confinement at shorter wavelengths and become increasingly delocalized at longer wavelengths.

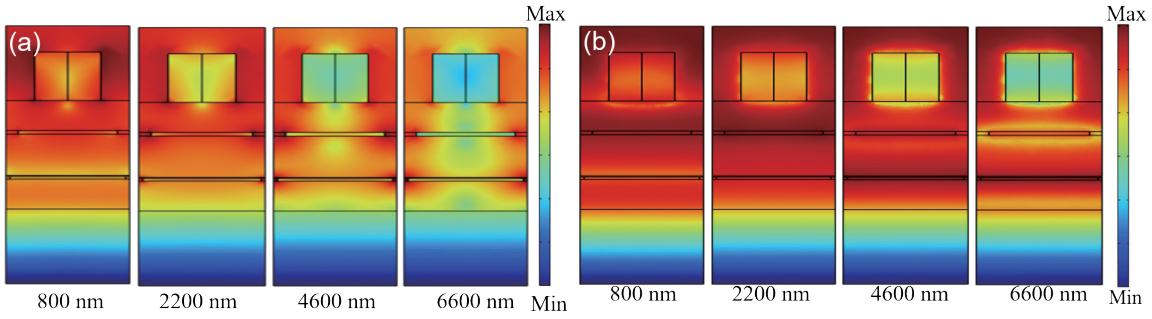

Fig. 7. (Color online) Distributions of (a) electric field and (b) magnetic field intensities of the proposed absorber under normal incidence at various TE-polarized wavelengths.

4. Conclusions

Simulation results revealed that the thicknesses of the h2 Cu_2O layer, h3 Fe layer, h5 Fe layer, and the h7 cylindrical Ti matrix significantly affected the absorption characteristics of the proposed multilayer metamaterial-based ultra-wideband absorber. For instance, increasing the thickness of the h2 Cu_2O layer within the range of 80–160 nm induced a redshift in the long-wavelength cutoff. Notably, when the h2 layer reached 120 nm, the absorber exhibited absorptivity exceeding 0.900 in both valley regions. The optimal thicknesses of the Fe layers (h1, h3, and h5) were determined to be 300, 10, and 15 nm, whereas those of the Cu_2O layers (h2, h4, and h6) were 120, 170, and 120 nm, respectively. Additionally, the optimal diameter and height of the h7 cylindrical Ti structure were found to be 160 and 195 nm, respectively. With these optimized parameters, the designed ultra-wideband absorber demonstrated high absorptivity over a wide spectral range, spanning from the VIS region (600 nm) to the MIR region (7250 nm).

Acknowledgments

This work was supported by Summit-Tech Resource Corp. and by projects under Nos. NSTC 113-2221-E-390-011 and NSTC 114-2622-E-390-001. We would be like to thank Pitotech Co. Ltd. for their help with the use of COMSOL Multiphysics® software.

References

1 S. Yanagi, A. Matsumoto, N. Toriumi, Y. Tanaka, K. Miyamoto, A. Muranaka, and M. Uchiyama: Angew. Chem. Int. Ed. **62** (2023) e202218358.
2 J. Haas and B. Mizaikoff: Annu. Rev. Anal. Chem. **9** (2016) 45.
3 L. V. Molina, R. C. Morales, J. Zhang, R. Schiek, I. Staude, A. A. Sukhorukov, and D. N. Neshev: Adv. Mater. **36** (2024) 2402777.
4 D. Honeybone, H. Peace, and M. Green: J. Mater. Chem. C **11** (2023) 7860.
5 A. S. Bhadoriya, V. Vegamoor, and S. Rathinam: Sensors **22** (2022) 4567.
6 A. Singh and R. Pal: Appl. Phys. A **123** (2017) 701.
7 J. J. Lin, L. C. Tseng, and C. F. Yang: Appl. Func. Mater. **3** (2023) 1.
8 D. Yang, L. C. Tseng, W. Z. Li, and C. F. Yang: Appl. Func. Mater. **3** (2023) 25.